Journal of Applied Nonlinear Dynamics

https://lhscientificpublishing.com/Journals/JAND-Default.aspx

Dynamics of three and four non-identical Josephson junctions

Alexander P. Kuznetsov, Igor R. Sataev, Yuliya V. Sedova†

Kotel'nikov's Institute of Radio-Engineering and Electronics of RAS, Saratov Branch, Zelenaya 38, Saratov, 410019, Russian Federation

Submission Info

Communicated by Referees
Received DAY MON YEAR
Accepted DAY MON YEAR
Available online DAY MON YEAR

Keywords

Josephson junctions
Resonance Arnold web
Lyapunov exponents chart

Abstract

Dynamics of chains of three and four coupled non-identical Josephson junctions is considered. Synchronization effects are discussed including resonance Arnold web formation on the base of tori of different dimensions.

The Josephson effect is widely used for generation and reception of very high frequency signals. Description of dynamics of several Josephson junctions included in the joint chain under certain conditions leads to the coupled phase oscillators - coupled Adler equations [1, 2]. Usually, the authors discuss junctions that are identical on critical currents. The case of two non-identical junctions is considered in [3]. The authors discuss the emerging two-dimensional tori, the phenomenon of junctions locking and structure of devil's staircase. In [4] the large arrays of junctions connected in groups with the same critical current are examined. Coupled oscillators with nonlinearity of sinus similar to Josephson junctions were discussed also in the context of design of generators of chaos in [5].

In this letter we study the array of three and four non-identical junctions. From the point of view of synchronization theory in such arrays the typical phenomenon is the possibility of invariant tori of different dimensions. This problem becomes the subject of our analysis.

Equations for the chain of coupled Josephson junction with parallel RCL-load may be written in the next form [1–4]:

$$\begin{aligned}&\tfrac{\hbar}{2er}\dot{\varphi}_n + I_n \sin\varphi_n = I - \dot{Q},\\ &L\ddot{Q} + R\dot{Q} + Q/C = \tfrac{\hbar}{2e}\sum_{n=1}^{N}\dot{\varphi}_n.\end{aligned} \tag{1}$$

Here φ_n are the junction phases and Q is the load capacitor charge, N is the number of junctions, $\hbar$ is Planck's constant, e is electron charge, $I_n \sin\varphi_n$ is superconducting current, I_n is a critical current through the corresponding junction with the resistance r, I is the external current, R, L, C are the elements of circuit including junctions, $\dot{Q}$ is the current through parallel RCL-load.

†Corresponding author.
Email address:sedovayv@yandex.ru

The first equation (1) describes the n-th contact, and the second one is the Kirchhoff equation for an electrical circuit, which includes junctions. It is convenient to renormalize variables to obtain the following dimensionless equation [4]:

$$\begin{aligned} &\dot{\varphi}_n = I - I_n \sin\varphi_n - \varepsilon\dot{Q}, \\ &\ddot{Q} + \gamma\dot{Q} + \omega_0^2 Q = I - \tfrac{1}{N}\sum_{n=1}^{N} I_n \sin\varphi_n. \end{aligned} \tag{2}$$

Further we assume that contacts are not identical on critical currents, so in accordance with [4] we obtain

$$\begin{aligned} &\dot{\varphi}_n = I - I_n \sin\varphi_n - \varepsilon\dot{Q}, \\ &\ddot{Q} + \gamma\dot{Q} + \omega_0^2 Q = I - \tfrac{1}{N}\sum_{n=1}^{N} (1+\xi_n) \sin\varphi_n. \end{aligned} \tag{3}$$

Here ξ_n is the parameter characterizing non-identity regarding critical currents. By its physical meaning $\xi_n > -1$ and the case $\xi_n = 0$ corresponds to identical junctions.

For three junctions ($N = 3$) with non-identical critical currents from (3) we have:

$$\begin{aligned} &\dot{\varphi}_1 = I - \sin\varphi_1 - \varepsilon\dot{Q}, \\ &\dot{\varphi}_2 = I - (1+\xi_1)\sin\varphi_2 - \varepsilon\dot{Q}, \\ &\dot{\varphi}_3 = I - (1+\xi_2)\sin\varphi_3 - \varepsilon\dot{Q}, \\ &\ddot{Q} + \gamma\dot{Q} + \omega_0^2 Q = I - \tfrac{1}{3}[\sin\varphi_1 + (1+\xi_1)\sin\varphi_2 + (1+\xi_2)\sin\varphi_3]. \end{aligned} \tag{4}$$

Further we will use the same parameters as in [4]: ε=0.5, γ=1, $\omega_0^2 = 1.2$.

From (4) it is easy to obtain an equilibrium state, assuming the time derivatives equal to zero:

$$\begin{aligned} &0 = I - \sin\varphi_1 \\ &0 = I - (1+\xi_1)\sin\varphi_2, \\ &0 = I - (1+\xi_2)\sin\varphi_3. \end{aligned} \tag{5}$$

Thus, the conditions of equilibrium existence are

$$I < 1,\ \xi_1 > I - 1,\ \xi_2 > I - 1. \tag{6}$$

Let us now numerically investigate the non-identity parameters plane(ξ_1, ξ_2) with the help of method of Lyapunov exponents charts [6–8]. At each point of the parameters plane we calculate a spectrum of Lyapunov exponents[a]. Then each point on the plane is painted in different colors to visualize the periodic regimes P, quasi-periodic regimes T2 and T3 corresponding to 2-tori and 3-tori, and chaos C according to the rules described in [7, 8]. At the top of Fig.1 we show the color palette corresponding to the type of regime determined by values of Lyapunov exponents.

At first let us to consider the case $I < 1$. The corresponding chart for $I = 0.8$ is shown in Fig.1a. In this case the structure of parameter plane in the area of two-frequency tori T2 contains the tongues of the different resonance periodic regimes and is qualitatively similar to the case of two junctions [3]. Gray color and abbreviation "eq" corresponds to a stable equilibrium (a kind of oscillations death effect [11]), which satisfies the conditions (5).

For parameter value $I = 1.1$ the picture significantly changes (Fig.1b). Especially transformations are notable in the left bottom part of the picture. This area is now represented mainly by three-dimensional tori. In the centre of mentioned area we can see the island of the periodic regime, which is

[a] Lyapunov exponents were estimated by the Benettin method [9]. Numerical solutions of the equations (3) and (4) were obtained with the help of the Dormand - Prince integrator [10], which uses the Runge - Kutta method of order 8 with an adaptive stepsize control. The local accuracy of integration while calculating the exponents was chosen to be 10^{-10}.

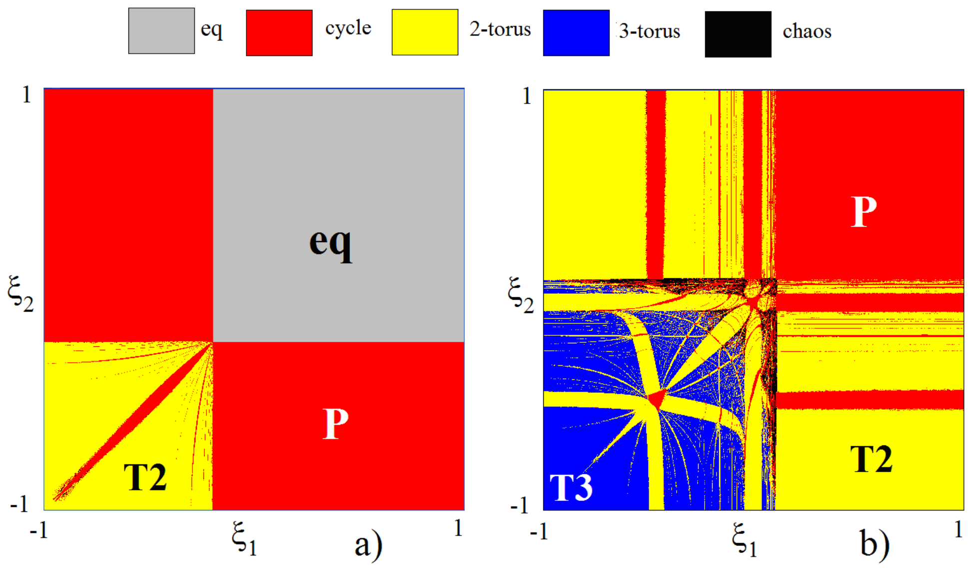

Fig. 1 Plane of nonidentity parameters for three junctions at ε=0.5, γ=1, $\omega_0^2 = 1.2$, a) $I = 0.8$, b) I=1.1.

shown in enlarged view in Fig.2a. Also there are the specific bands of two-frequency regimes, radiating like a fan from the regions of periodic mode. Another interesting fragment is shown in Fig.2b. It can be characterized as resonance Arnold web, which is one of the important illustrations of multi-frequency dynamics [6–8]. The chart demonstrates a lot of thin strips (the web) of two-frequency regimes, which, being crossed, generate many small islands of periodic regimes.

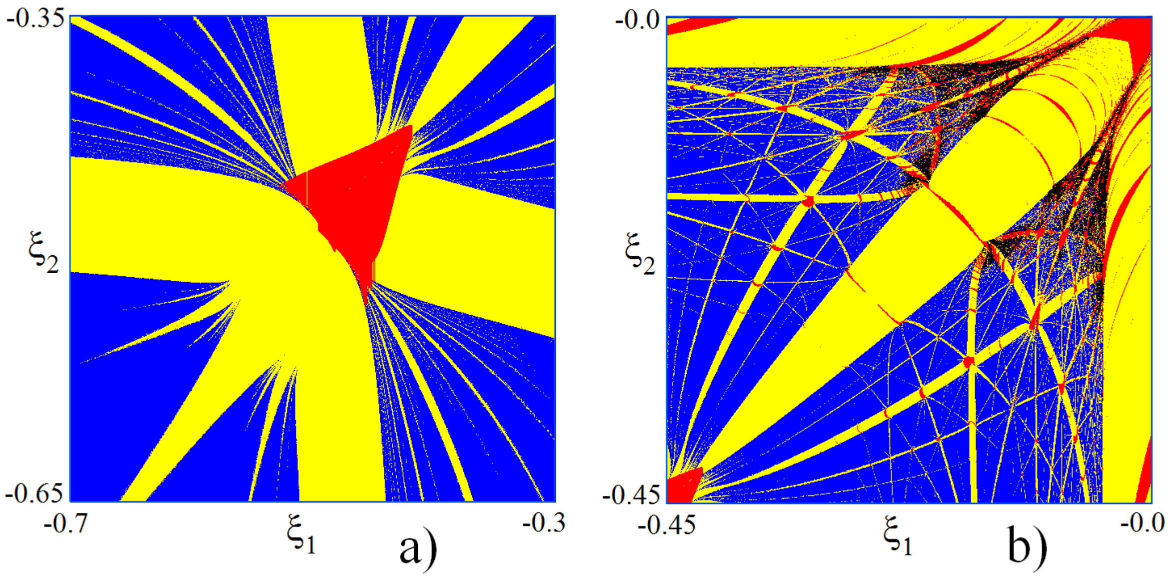

Fig. 2 Enlarged fragments of Fig.1b.

In Fig.3 we reproduce the parameter plane of Fig.1b and present three-dimensional phase portraits in selected points.

Let us construct a kind of extended phase portraits using not only the phase variables, but also the variable Q. Examples for periodic regime, 2-torus, 3-torus and chaos are given in Fig.4 (points 6,

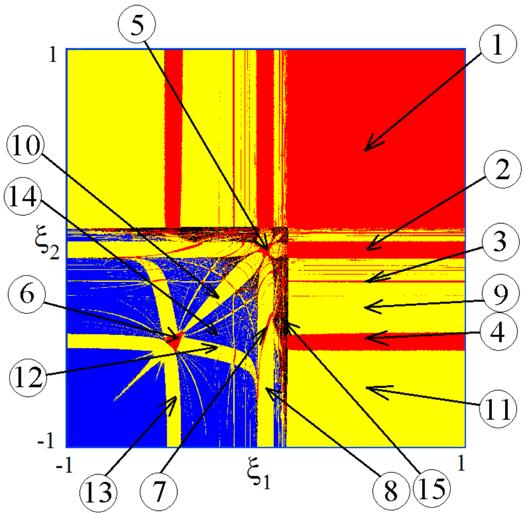

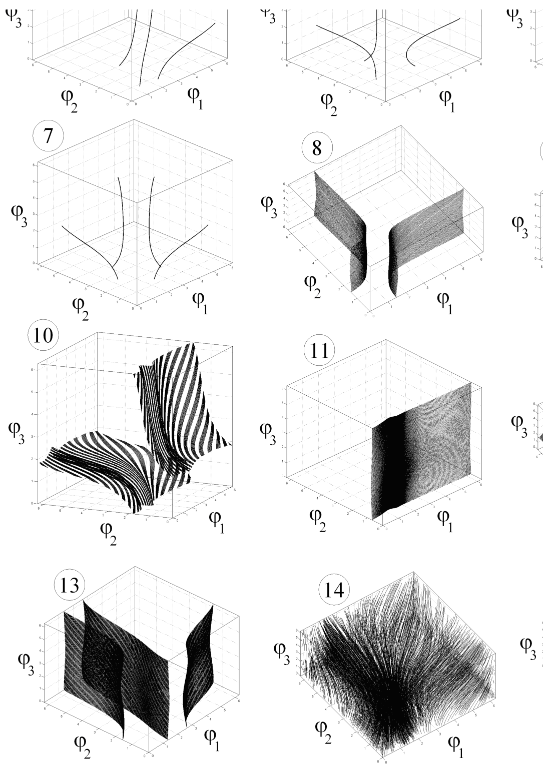

Fig. 3 Phase portraits in selected points of parameter plane.

12, 14 and 15 in the parameter plane of Fig.3). Some distinctive features of 2-tori, 3-tori and chaos are visible. It is obvious that in such figure it is difficult to distinguish visually the 3-torus and chaos. For example, in the bottom part of Fig.4 we show the resonant 3-torus located very close to the point demonstrating chaos.

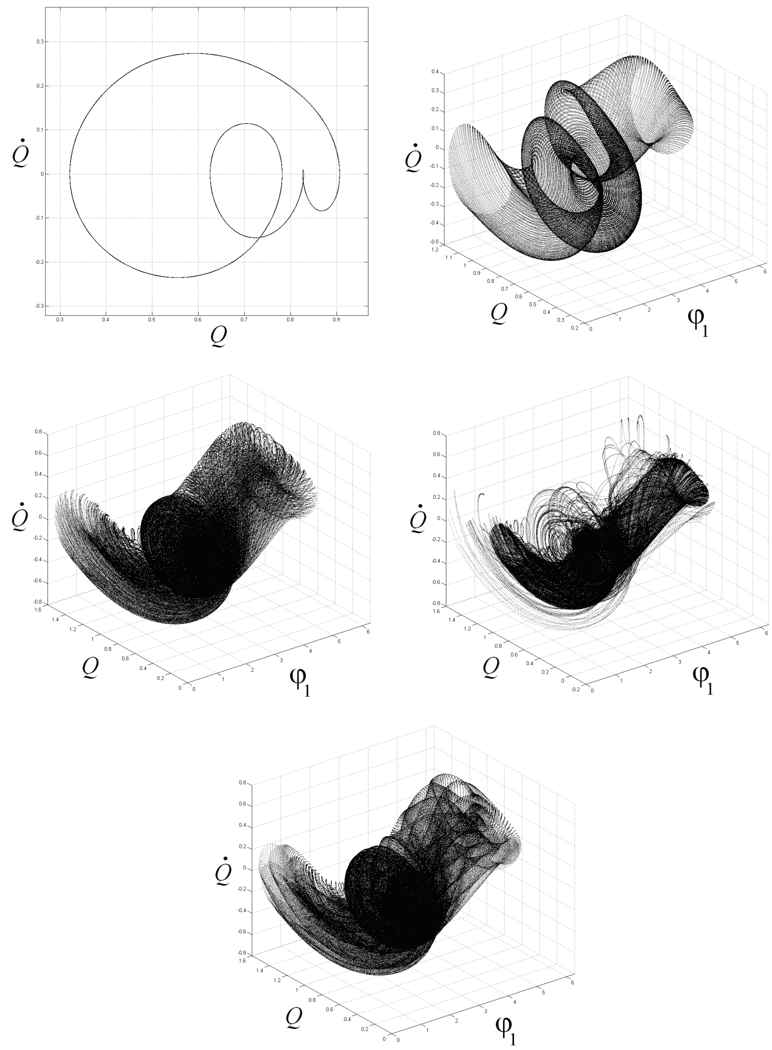

Fig. 4 Phase portraits in extended phase space.

For four junctions from (3) we get the next system of equations:

$$
\begin{aligned}
&\dot{\varphi}_1 = I - \sin\varphi_1 - \varepsilon\dot{Q},\\
&\dot{\varphi}_2 = I - (1+\xi_1)\sin\varphi_2 - \varepsilon\dot{Q},\\
&\dot{\varphi}_3 = I - (1+\xi_2)\sin\varphi_3 - \varepsilon\dot{Q},\\
&\varphi_4 = I - (1+\xi_3)\sin\varphi_4 - \varepsilon\dot{Q},\\
&\ddot{Q} + \gamma\dot{Q} + \omega_0^2 Q = I - \tfrac{1}{4}[\sin\varphi_1 + (1+\xi_1)\sin\varphi_2 + (1+\xi_2)\sin\varphi_3 + (1+\xi_3)\sin\varphi_4].
\end{aligned}
\tag{7}
$$

Let us apply for calculations previously used values of parameters: ε=0.5, γ=1, $\omega_0^2 = 1.2$. For critical current we fix I=1.1. In accordance with Fig.1b the value $\xi_1 = -0.25$ from three-frequency quasi-periodical area is chosen. The calculated Lyapunov exponent chart on the plane (ξ_2, ξ_3) is demonstrated in Fig.5.

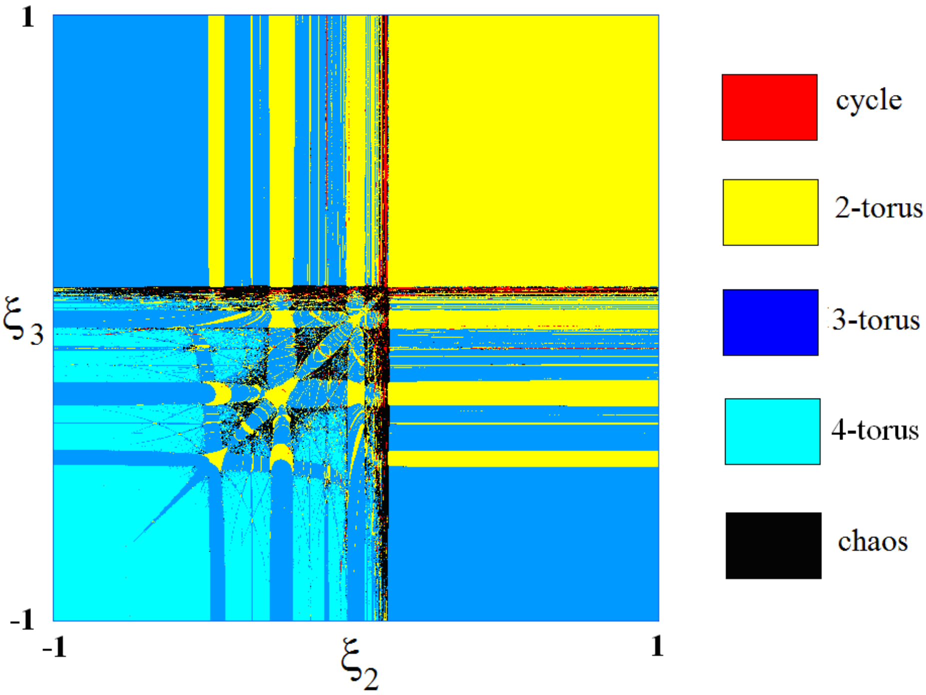

Fig. 5 Lyapunov exponent chart for four non-identical junctions (7).

In this case the resonance Arnold web is visualized on basis of 4-tori. At the intersection of the three-frequency regimes bands the islands of 2-tori are located. The number of bands is more than in Fig.1b. Accordingly, now chaos is observed much more frequently in the vicinity of overlapping bands.

Thus, even three and four non-identical Josephson junctions can exhibit quite complex behavior, including resonance Arnold web on the base of the tori of different dimensions.

This research was partly supported by the Russian Foundation for Basic Research (grants 14-02-00085, 16-02-00135).

References

[1] Pikovsky, A., Rosenblum, M. and Kurths, J. (2001) *Synchronization. A Universal Concept in Nonlinear Sciences*, Cambridge University Press.

[2] Wiesenfeld, K., Colet, P., Strogatz, S.H. (1996), Synchronization transitions in a disordered Josephson series array, *Phys. Rev. Lett.*, **76**, 404–407.

[3] Valkering, T.P., Hooijer, C.L.A., Kroon, M.F. (2000), Dynamics of two capacitively coupled Josephson junctions in the overdamped limit, *Physica D: Nonlinear Phenomena*, **135**, 137–153.

[4] Vlasov, V, Pikovsky, A. (2013), Synchronization of a Josephson junction array in terms of global variables, *Phys. Rev. E*, **88**, 022908.

[5] Kuznetsov, S.P. (2016), From geodesic flow on a surface of negative curvature to electronic generator of robust chaos, *Int. J. Bifurcation Chaos*, **26**, 1650232.

[6] Baesens, C., Guckenheimer, J., Kim, S. and MacKay, R.S. (1991) Three coupled oscillators: mode locking, global bifurcations and toroidal chaos, *Physica D: Nonlinear Phenomena*, **49**, 387-475.

[7] Emelianova, Yu.P., Kuznetsov, A.P., Sataev, I.R. and Turukina, L.V.(2013) Synchronization and multi-frequency oscillations in the low-dimensional chain of the self-oscillators, *Physica D: Nonlinear Phenomena*, **244**, 36-49.

[8] Emelianova, Y.P., Kuznetsov, A.P., Turukina, L.V., Sataev, I.R. and Chernyshov, N.Yu. (2014) A structure of the oscillation frequencies parameter space for the system of dissipatively coupled oscillators, *Communications*

in Nonlinear Science and Numerical Simulation, **19**, 1203-1212.

[9] Benettin, G., Galgani, L., Giorgilli, A. and Strelcyn, J.-M. (1980) Lyapunov Characteristic Exponents for Smooth Dynamical Systems and for Hamiltonian Systems: A Method for Computing All of Them: P. 1: Theory; P. 2: Numerical Application, *Meccanica*, **15**, 9-30.

[10] Hairer, E., Norsett., S.P. and Wanner, G. (1987) *Solving Ordinary Differential Equations: 1. Nonstiff Problems*, Berlin: Springer.

[11] Aronson, D.G., Ermentrout, G.B., Kopell, N. (1990) Amplitude response of coupled oscillators, *Physica D: Nonlinear Phenomena*, **41**, 403-449.